Inflammation at the tissue-electrode interface in a case of rapid deterioration in hearing performance leading to explant after cochlear implantation

Running title: Understanding soft failure after cochlear implantation

Kate Hough[1*], MBiomed., Alan Sanderson[1*], MSc., Mary Grasmeder[2], PhD, Tim Mitchell[2] FRCS, Carl A Verschuur[2] PhD., Tracey A Newman[3], PhD.,

[1]Faculty of Engineering and Physical Sciences, University of Southampton, U.K.

[2]Faculty of Engineering and Physical Sciences, Auditory Implant Centre, University of Southampton, U.K.

[3]Clinical and Experimental Sciences, Faculty of Medicine, IfLS, University of Southampton, U.K.,

*these authors contributed equally to this work

Corresponding author:

Tracey A Newman, B85, Life Sciences, Faculty of Medicine, University Road,

Southampton, Hants,

UK SO17 1BJ.

Tel: 0044-2380597642

email: t.a.newman@soton.ac.uk

Sources of funding: EPSRC for PhD studentship funding to K Hough and A Sanderson

Conflict of interest: The authors declare that there are no conflicts of interest associated with this report.

Authorship: All authors listed meet the criteria for having contributed to the production of this manuscript.

Introduction A small but persistent percentage of cases fail to achieve or maintain the desired hearing outcomes after cochlear implantation (1,2). Soft failure is indicated by a broad assessment battery that allows hardware and medical failures to be ruled out (3). Some soft failures are due to tissue responses to the CI that develop over time (4-6). Surgical trauma, electrode style (7), electrode materials and anti-inflammatory steroid treatment (8,9) all influence the tissue response. However, the mechanisms of this immune-mediated homeostatic response to implantation are inherently difficult to study in people. This case report describes the performance measures across the period of implantation, and histology of the tissue response at the electrode array, in a case where rapid electrode migration necessitated explantation and re-implantation. This work gives unique insight into the developmental time course of ~~intracochlear~~ tissue associated with the array during performance changes. Findings add to the existing knowledge gained through post-mortem analyses (4,5,10,11) and provide the basis for a feasible protocol for a larger, systematic analysis of soft failures with the aim of reducing the need for explantation.

The individual who has a history of autoimmune disease developed a progressive sensorineural hearing loss over a decade. She was implanted in her early fifties by which time her hearing loss was profound for frequencies of 2 kHz and above ~~by~~ and ~~only~~ moderate for low frequencies (250 and 500 Hz). Audiometry and speech perception scores met the guidelines for funding for cochlear implantation in the UK and a Nucleus CI522 device was fully inserted through the round window, confirmed by post-operative x-ray, using a hearing preservation technique, including application of steroids. Vicryl ties were used to anchor the electrode array and receiver stimulator, muscle was used to seal the array in the round window. The device was activated six weeks later using the ACE processing strategy with a stimulation rate of 900 Hz, pulse width of 37 µs, 10 maxima and stimulation mode MP1+2. At activation there were only limited changes in audiometric thresholds compared to pre-operative levels: the audiometric thresholds at 250 and 500 Hz were 65 and 80 dBHL, compared to 60 dBHL for these frequencies pre-operatively. However, the two most basal electrodes (E1 and E2) gave open circuits on impedance telemetry and so were deactivated. The

remaining electrodes had impedances within the normal range. Stimulation threshold measurements were higher for electrodes 3 to 5 (>120 Nucleus current units) than for more apical electrodes (70-80 Nucleus current units). Over ten months, successive basal electrodes within the cochlea were deactivated (Figure 1a) due to measures consistent with open circuits, reports of non-auditory sensations, poor loudness growth and drop in speech perception scores for BKB sentences in quiet (Figure 1a). Rapid and dramatic (Figure 1b) increases in impedance were measured over time. The clinical profile suggested electrode migration, which was confirmed by a CT scan 3-months post activation (Figure 1c-e). Consequently, ten months after implantation the decision was made to explant and replace with a new device. At explantation the surgeon reported significant fibrosis and mechanical resistance to array removal and observed five extra-cochlear electrodes. A fibrotic sheath was seen (Figure 2a) on the array. Routine hardware testing confirmed that the device was functional. Accordingly, the case was diagnosed as a soft failure. The patient consented to an investigation of the tissue associated with the device and to the use of their fully anonymised data in this case report.

Method To determine the cellular response to the electrode array in the tissue seen at time of explantation. On removal the device was prepared for histological analysis by tissue fixation in 10% neutral buffered formalin, prior to immersion in 70% ethanol (v/v). A midline incision was made along the length of the tissue cuff (figure 2a), the tissue removed and immersed in 30% sucrose in 0.1% phosphate buffer for cryoprotection prior to embedding in OCT (Finntek) (12). The device was returned to the manufacturer for integrity testing. Tissue sections (10 μm) were cut using a cryostat (Leica) and collected onto APES coated (13) glass slides. To reveal the gross morphology and cellular organisation tissue sections collected at four equidistant points (Figure 2a,b) along the cuff were stained using haematoxylin and eosin (Harris) and MSB trichrome. Immunohistochemistry (see supplementary table 1 for detail) was used to identify macrophages, T cells, interleukin-1,β proliferating cells and blood vessels(6,14). Endogenous peroxidase was quenched using 1% hydrogen peroxide. Biotinylated secondary antibodies were labelled using streptavidin conjugated horse-

radish peroxidase (HRP) detected using diaminobenzidine. Sections were counterstained using haematoxylin, dehydrated through serial alcohols, cover-slipped using DPX mounting media and air-dried overnight. Images were captured using light microscopy (Q-imaging 2000R digital camera connected to a Nikon eclipse E4000 microscope and Nikon HB-101004F light source).

Results The four basal electrodes were encapsulated in fibrotic tissue. Beyond this the cuff of fibrotic tissue appeared to have sheared (figure 2a, asterisk) at the round window niche on ~~explantation, poss~~ibly reflecting which may be consistent with the resistance to removal noted in the surgical report. The tissue was composed of a heterogeneous mix of cells and extracellular matrix protein across and within the four regions examined (Figure 2c-f) with an increase in cellularity closest to the round window. Stratification and organisation of the cells within the tissue cuff is clear as seen in figure 2e-k. Eosinophils and neutrophils, evidence of active inflammation (15), can be seen in figure 2l,m. Collagen deposition differs across the tissue with the spatial organisation of the collagen across and within regions suggesting different stages of tissue maturity and potential functional differences (16). Immunohistochemical analysis of the tissue identified CD68-positive cells (Figure 3a) at the edge of the tissue in close proximity to the position of the electrode array. Interleukin-1β expression, evidence of inflammatory signalling between cells, (17) is seen (figure 3b). A second macrophage (CD163+ve) population (18) was observed in low numbers (relative to the CD68+ve population) largely around the perimeter of the tissue sections (figure 3c). Clusters of T cells (Figure 3d) were observed in region 4, most distant from the electrode surface. Evidence of active cell (Figure 4a, Ki67 expression) and vascular proliferation identified by expression of vascular endothelial growth factor receptor 2 (Figure 4b) was seen in regions of the tissue. Alpha smooth muscle actin was clearly associated with vessels (Figure 4c) and in cells within the regions of connective tissue (Figure 4d).

Discussion Tissue growth (fibrosis) at the electrode-cochlear interface in this case is associated with an ascending pattern of sequential open circuits starting at the basal end, altered impedance measures and an associated drop in BKB sentence scores in quiet. Sequential deactivation of electrodes began at switch-on and continued across the subsequent clinic visits. Macrophages,

neutrophils and interleukin-1 βexpression identified in the fibrotic tissue on the array are consistent with a chronic inflammatory (19) response i.e. one that has not resolved despite the length of time (10 months) since implantation. Whether this aberrant response is contributory to the migration of the array, or a consequence of repeated tissue remodelling due to movement of the array, cannot be determined. Typically, cell-signalling during the time after implantation, the acute phase, would mediate wound repair and progress to a collagen-rich dominated response with sparse macrophages at the site expressing anti-inflammatory mediators consistent with a restoration of homeostasis
(12,20).The expression of vascular growth factor receptors (VEGF2R) (21) and upregulation of proliferation marker (Ki67) (22) support the active state of the tissue. As the use of implants becomes more common across different organs and tissues e.g. cochlear implants, vascular stents, and joint prostheses, there is a growing recognition that the immune response to the implant may contribute to complications, or impaired function of the implant (23,24). Whether this is due to the immune response to a particular material is unclear. It is also unclear whether the response to a material varies between individuals, or even within an individual, according to other co-existent conditions (25). This may be relevant in this case in which the individual was implanted with a Nucleus CI512 device immediately after the explantation of the migrated device. Explantation was made difficult by the presence of fibrotic tissue, but a full insertion was achieved on re-implantation. Significantly, tuning of the new device was straightforward and only the most basal electrode was deactivated. After one year of use of the new device, there are no indications of electrode migration and all impedances are in the normal range. Auditory performance has exceeded levels obtained early on with the first implant with 99% correct on the BKB sentence test in quiet and 2.0dB in adaptive noise

Conclusions This is the first report to combine (i) post-cochlear implant cochlear tissue analysis from a person who has subsequently been re-implanted, (ii) the tissue is from a relatively early stage post-implantation (particularly when compared to the majority of cadaveric cases) and (iii) the histology is considered in the context of the functional outcomes and clinical history around time of

explantation. The determines that investigation of fibrosis on explanted devices from living cases is feasible. The tissue response to implanted arrays is known to be associated with cases of poor performance (26) but little is known about whether clear biomarkers of a detrimental fibrotic response can be identified. There is a need to reduce soft failures, due to the surgical and psychological burden on the person with the implant and the associated healthcare costs (27). By investigating cases that undergo subsequent re-implantation it may be possible to determine the likelihood that a detrimental response to implantation is due to the individual or to some aspect of the implantation process. The establishment of a profile of the immune responses to the implant over time after implantation (such as could be obtained from a population of explanted devices) may identify targets for immune-modulation that could increase the useful lifetime of individual implants.

1. Venail F, Sicard M, Piron JPet al. Reliability and complications of 500 consecutive cochlear implantations. *Archives of Otolaryngology - Head and Neck Surgery* 2008;134:1276-81.
2. Causon A, Verschuur C, Newman TA. Trends in cochlear implant complications: implications for improving long-term outcomes. *Otol Neurotol* 2013;34:259-65.
3. Bourdoncle M, Fargeot C, Poncet Cet al. Analysis and management of cochlear implant explantation in adults. *Eur Ann Otorhinolaryngol Head Neck Dis* 2020.
4. Nadol JB, Eddington DK, Burgess BJ. Foreign Body or Hypersensitivity Granuloma of the Inner Ear After Cochlear Implantation: One Possible Cause of a Soft Failure? *Otology and Neurotology* 2008;29:1076-84.
5. Seyyedi M, Nadol JB. Intracochlear Inflammatory Response to Cochlear Implant Electrodes in Humans. *Otology & Neurotology* 2014;35:1545-51.
6. Nadol JB, O'Malley JT, Burgess BJet al. Cellular immunologic responses to cochlear implantation in the human. *Hearing Research* 2014;318:11-7.
7. Ishai R, Herrmann BS, Nadol JBet al. The pattern and degree of capsular fibrous sheaths surrounding cochlear electrode arrays. *Hearing Research* 2017;348:44-53.
8. Bas E, Bohorquez J, Goncalves Set al. Electrode array-eluted dexamethasone protects against electrode insertion trauma induced hearing and hair cell losses, damage to neural elements, increases in impedance and fibrosis: A dose response study. *Hearing Research* 2016;337:12-24.
9. Needham K, Stathopoulos D, Newbold Cet al. Electrode impedance changes after implantation of a dexamethasone-eluting intracochlear array. *Cochlear Implants International* 2019;0:1-12.

10. Kamakura T, O'Malley JT, Nadol JB. Preservation of Cells of the Organ of Corti and Innervating Dendritic Processes Following Cochlear Implantation in the Human: An Immunohistochemical Study. *Otology and Neurotology* 2018;39:284-93.
11. Okayasu T, Quesnel AM, O'Malley JTet al. The Distribution and Prevalence of Macrophages in the Cochlea Following Cochlear Implantation in the Human: An Immunohistochemical Study Using Anti-Iba1 Antibody. *Otol Neurotol* 2020;41:e304-e16.
12. Bas E, Goncalves S, Adams Met al. Spiral ganglion cells and macrophages initiate neuro-inflammation and scarring following cochlear implantation. *Frontiers in Cellular Neuroscience* 2015;9.
13. Maddox PH, Jenkins D. 3-Aminopropyltriethoxysilane (APES): a new advance in section adhesion. *Journal of clinical pathology* 1987;40:1256-60.
14. Moreno B, Jukes JP, Vergara-Irigaray Net al. Systemic inflammation induces axon injury during brain inflammation. *Ann Neurol* 2011;70:932-42.
15. Christo SN, Diener KR, Bachhuka Aet al. Innate Immunity and Biomaterials at the Nexus: Friends or Foes. *BioMed Research International* 2015;2015.
16. Coelho NM, McCulloch CA. Contribution of collagen adhesion receptors to tissue fibrosis. *Cell Tissue Res* 2016;365:521-38.
17. Landgraeber S, Jäger M, Jacobs JJet al. The pathology of orthopedic implant failure is mediated by innate immune system cytokines. *Mediators Inflamm* 2014;2014:185150.
18. Galea I, Felton LM, Waters Set al. Immune-to-brain signalling: the role of cerebral CD163-positive macrophages. *Neurosci Lett* 2008;448:41-6.
19. Kzhyshkowska J, Gudima A, Riabov Vet al. Macrophage responses to implants: prospects for personalized medicine. *Journal of Leukocyte Biology* 2015;98:953-62.
20. Gurtner GC, Werner S, Barrandon Yet al. Wound repair and regeneration. *Nature* 2008;453:314-21.
21. Kendall RT, Feghali-Bostwick CA. Fibroblasts in fibrosis: Novel roles and mediators. *Frontiers in Pharmacology* 2014;5 MAY:1-13.
22. Sun X, Kaufman PD. Ki-67: more than a proliferation marker. *Chromosoma* 2018;127:175-86.
23. Anderson JM, Rodriguez A, Chang DT. Foreign body reaction to biomaterials. *Seminars in Immunology* 2008;20:86-100.
24. Mariani E, Lisignoli G, Borzì RMet al. Biomaterials: Foreign bodies or tuners for the immune response? *International Journal of Molecular Sciences* 2019;20.
25. Chung D, Kim AH, Parisier Set al. Revision cochlear implant surgery in patients with suspected soft failures. *Otology and Neurotology* 2010;31:1194-8.
26. Foggia MJ, Quevedo RV, Hansen MR. Intracochlear fibrosis and the foreign body response to cochlear implant biomaterials. *Laryngoscope Investig Otolaryngol* 2019;4:678-83.
27. Crowson MG, Semenov YR, Tucci DLet al. Quality of Life and Cost-Effectiveness of Cochlear Implants: A Narrative Review. *Audiol Neurootol* 2017;22:236-58.

Figure legends

Figure 1 *Clinical indicators of electrode migration concomitant with a deterioration in hearing.*

A. Electrode status and speech recognition scores over time. Scores for the BKB sentence test (in quiet) are shown for the cochlear implant alone (black line) and the hybrid (grey line) device [combined acoustic and electrical stimulation] post-implant. **B**. Impedance telemetry in common ground mode from activation until shortly prior to re-implantation. **C**. X-ray micrograph obtained 1-day post-implantation showing the intra-cochlear position of the electrode array. **D.** Electrode contact positions superimposed (black). **E**. Cochlear template adapted from Kawano et al 1996, defining the position of every quarter turn of the Organ of Corti, showing the points from the basal turn. The position of the electrode array post-implantation superimposed (black) based on the post-operative x-ray and the expected position of the migrated array before explantation superimposed (white) – showing four extra-cochlear electrodes.

Figure 2. *Explanted electrode with associated fibrotic tissue prior to tissue removal and after sectioning and histochemical staining to illustrate the variable cellular response and local organisation within the fibrotic tissue.*

Photographs of the full length of electrode array (**A**) showing fibrotic tissue enveloping the basal portion of the array. The insert in (A) identifies the four regions of tissue referred to in subsequent images and is shown at higher magnification in **B,** where the black arrows indicate tissue-covered electrode contacts and the numbers refer to the regions in C-F. **C-F** Low magnification (x4) images of sections representative of regions 1 to 4 respectively to illustrate the gross organisation of the tissue along its length. **G-N,** higher magnification (x40) images showing the variability in density of cells and volume of connective tissue across and within the regions. **G and H,** illustrate areas of loose connective tissue with sparsely distributed cells. **I** areas of dense, organised cells close to position of the electrode array. **J,** areas packed with cell nuclei and and dense connective tissue in **K** with aligned collagen fibres. **L-N,** inflammatory cells (arrows) including eosinophils (**L**), neutrophils (**M**), and foreign body giant cells (**N)**. Histochemical stains; haematoxylin and eosin, except G, K which are stained using MSB trichrome. Scale bar: C - F = 200 µm, G - N = 10 µm.

Figure 3. *Variable expression of cellular markers of macrophages and T cells within the explant tissue.*

Light microscopy images of tissue sections immunolabelled using **A**. anti-CD68, a marker of phagocytic macrophages. CD68-positive cells were observed at the edges of the tissue in close proximity to where the array was in all four regions. **B**. Anti-Interleukin 1β, a pro-inflammatory cytokine. **C**. Anti-CD163 a marker of anti-inflammatory macrophages. CD163-positive macrophages were observed in lower number (compared to CD68) and were mostly observed around the perimeter of the tissue. **D**. T-lymphocytes labelled with anti-CD3. Clusters of T cells were observed in region 4 in tissue furthest away from the array. Arrows highlight examples of positively labelled cells. Scale bar: 10 μm.

Figure 4. *Evidence of active tissue proliferation and angiogenesis.*

Light microscopy images of tissue sections immunolabelled using **A**. Anti-Ki-67 a marker of dividing i.e. proliferating cells. The majority of the Ki-67 positive cells were observed in regions of low cell density and high extracellular matrix. **B**. Vascular endothelial growth factor receptor-2 (VEGFR2) a marker of developing blood vessels i.e. angiogenesis. VEGFR2 expression was primarily observed in regions distal to the electrode array. **C**. Expression of alpha-smooth muscle actin (α-sma) clearly associated with blood vessel walls and **in D** α-sma positive cells indicating myofibroblasts that do not appear to be associated with vessels. Examples of positively labelled cells are indicated by arrows. Scale bar: 10 μm.

Introduction A small but persistent percentage of cases fail to achieve or maintain the desired hearing outcomes after cochlear implantation (1,2). Soft failure is indicated by a broad assessment battery that allows hardware and medical failures to be ruled out (3). Some soft failures are due to tissue responses to the CI that develop over time (4-6). Surgical trauma, electrode style (7), electrode materials and anti-inflammatory steroid treatment (8,9) all influence the tissue response. However, the mechanisms of this immune-mediated homeostatic response to implantation are inherently difficult to study in people. This case report describes the performance measures across the period of implantation, and histology of the tissue response at the electrode array, in a case where rapid electrode migration necessitated explantation and re-implantation. This work gives unique insight into the developmental time course of ~~intracochlear~~ tissue associated with the array during performance changes. Findings add to the existing knowledge gained through post-mortem analyses (4,5,10,11) and provide the basis for a feasible protocol for a larger, systematic analysis of soft failures with the aim of reducing the need for explantation.

The individual who has a history of autoimmune disease developed a progressive sensorineural hearing loss over a decade. She was implanted in her early fifties by which time her hearing loss was profound for frequencies of 2 kHz and above and moderate for low frequencies (250 and 500 Hz). Audiometry and speech perception scores met the guidelines for funding for cochlear implantation in the UK and a Nucleus CI522 device was fully inserted through the round window, confirmed by post-operative x-ray, using a hearing preservation technique, including application of steroids. Vicryl ties were used to anchor the electrode array and receiver stimulator, muscle was used to seal the array in the round window. The device was activated six weeks later using the ACE processing strategy with a stimulation rate of 900 Hz, pulse width of 37 μs, 10 maxima and stimulation mode MP1+2. At activation there were only limited changes in audiometric thresholds compared to pre-operative levels: the audiometric thresholds at 250 and 500 Hz were 65 and 80 dBHL, compared to 60 dBHL for these frequencies pre-operatively. However, the two most basal electrodes (E1 and E2) gave open circuits on impedance telemetry and so were deactivated. The remaining electrodes had

impedances within the normal range. Stimulation threshold measurements were higher for electrodes 3 to 5 (>120 Nucleus current units) than for more apical electrodes (70-80 Nucleus current units). Over ten months, successive basal electrodes within the cochlea were deactivated (Figure 1a) due to measures consistent with open circuits, reports of non-auditory sensations, poor loudness growth and drop in speech perception scores for BKB sentences in quiet (Figure 1a). Rapid and dramatic (Figure 1b) increases in impedance were measured over time. The clinical profile suggested electrode migration, which was confirmed by a CT scan 3-months post activation (Figure 1c-e). Consequently, ten months after implantation the decision was made to explant and replace with a new device. At explantation the surgeon reported significant fibrosis and mechanical resistance to array removal and observed five extra-cochlear electrodes. A fibrotic sheath was seen (Figure 2a) on the array. Routine hardware testing confirmed that the device was functional. Accordingly, the case was diagnosed as a soft failure. The patient consented to an investigation of the tissue associated with the device and to the use of their fully anonymised data in this case report.

Method To determine the cellular response to the electrode array in the tissue seen at time of explantation. On removal the device was prepared for histological analysis by tissue fixation in 10% neutral buffered formalin, prior to immersion in 70% ethanol (v/v). A midline incision was made along the length of the tissue cuff (figure 2a), the tissue removed and immersed in 30% sucrose in 0.1% phosphate buffer for cryoprotection prior to embedding in OCT (Finntek) (12). The device was returned to the manufacturer for integrity testing. Tissue sections (10 μm) were cut using a cryostat (Leica) and collected onto APES coated (13) glass slides. To reveal the gross morphology and cellular organisation tissue sections collected at four equidistant points (Figure 2a,b) along the cuff were stained using haematoxylin and eosin (Harris) and MSB trichrome. Immunohistochemistry (see supplementary table 1 for detail) was used to identify macrophages, T cells, interleukin-1β, proliferating cells and blood vessels(6,14). Endogenous peroxidase was quenched using 1% hydrogen peroxide. Biotinylated secondary antibodies were labelled using streptavidin conjugated horse-

radish peroxidase (HRP) detected using diaminobenzidine. Sections were counterstained using haematoxylin, dehydrated through serial alcohols, cover-slipped using DPX mounting media and air-dried overnight. Images were captured using light microscopy (Q-imaging 2000R digital camera connected to a Nikon eclipse E4000 microscope and Nikon HB-101004F light source).

Results The four basal electrodes were encapsulated in fibrotic tissue. Beyond this the cuff of fibrotic tissue appeared to have sheared (figure 2a, asterisk) at the round window niche on explantation, which is consistent with the resistance to removal noted in the surgical report. The tissue was composed of a heterogeneous mix of cells and extracellular matrix protein across and within the four regions examined (Figure 2c-f) with an increase in cellularity closest to the round window. Stratification and organisation of the cells within the tissue cuff is clear as seen in figure 2e-k. Eosinophils and neutrophils, evidence of active inflammation (15), can be seen in figure 2l,m. Collagen deposition differs across the tissue with the spatial organisation of the collagen across and within regions suggesting different stages of tissue maturity and potential functional differences (16). Immunohistochemical analysis of the tissue identified CD68-positive cells (Figure 3a) at the edge of the tissue in close proximity to the position of the electrode array. Interleukin-1β expression, evidence of inflammatory signalling between cells, (17) is seen (figure 3b). A second macrophage (CD163+ve) population (18) was observed in low numbers (relative to the CD68+ve population) largely around the perimeter of the tissue sections (figure 3c). Clusters of T cells (Figure 3d) were observed in region 4, most distant from the electrode surface. Evidence of active cell (Figure 4a, Ki67 expression) and vascular proliferation identified by expression of vascular endothelial growth factor receptor 2 (Figure 4b) was seen in regions of the tissue. Alpha smooth muscle actin was clearly associated with vessels (Figure 4c) and in cells within the regions of connective tissue (Figure 4d).

Discussion Tissue growth (fibrosis) at the electrode-cochlear interface in this case is associated with an ascending pattern of sequential open circuits starting at the basal end, altered impedance measures and an associated drop in BKB sentence scores in quiet. Sequential deactivation of electrodes began at switch-on and continued across the subsequent clinic visits. Macrophages,

neutrophils and interleukin-1β expression identified in the fibrotic tissue on the array are consistent with a chronic inflammatory (19) response i.e. one that has not resolved despite the length of time (10 months) since implantation. Whether this aberrant response is contributory to the migration of the array, or a consequence of repeated tissue remodelling due to movement of the array, cannot be determined. Typically, cell-signalling during the time after implantation, the acute phase, would mediate wound repair and progress to a collagen-rich dominated response with sparse macrophages at the site expressing anti-inflammatory mediators consistent with a restoration of homeostasis (12,20).The expression of vascular growth factor receptors (VEGF2R) (21) and upregulation of proliferation marker (Ki67) (22) support the active state of the tissue. As the use of implants becomes more common across different organs and tissues e.g. cochlear implants, vascular stents, and joint prostheses, there is a growing recognition that the immune response to the implant may contribute to complications, or impaired function of the implant (23,24). Whether this is due to the immune response to a particular material is unclear. It is also unclear whether the response to a material varies between individuals, or even within an individual, according to other co-existent conditions (25). This may be relevant in this case in which the individual was implanted with a Nucleus CI512 device immediately after the explantation of the migrated device. Explantation was made difficult by the presence of fibrotic tissue, but a full insertion was achieved on re-implantation. Significantly, tuning of the new device was straightforward and only the most basal electrode was deactivated. After one year of use of the new device, there are no indications of electrode migration and all impedances are in the normal range. Auditory performance has exceeded levels obtained early on with the first implant with 99% correct on the BKB sentence test in quiet and 2.0dB in adaptive noise

Conclusions This is the first report to combine (i) post-cochlear implant cochlear tissue analysis from a person who has subsequently been re-implanted, (ii) the tissue is from a relatively early stage post-implantation (particularly when compared to the majority of cadaveric cases) and (iii) the histology is considered in the context of the functional outcomes and clinical history around time of

explantation. This determines that investigation of fibrosis on explanted devices from living cases is feasible. The tissue response to implanted arrays is known to be associated with cases of poor performance (26) but little is known about whether clear biomarkers of a detrimental fibrotic response can be identified. There is a need to reduce soft failures, due to the surgical and psychological burden on the person with the implant and the associated healthcare costs (27). By investigating cases that undergo subsequent re-implantation it may be possible to determine the likelihood that a detrimental response to implantation is due to the individual or to some aspect of the implantation process. The establishment of a profile of the immune responses to the implant over time after implantation (such as could be obtained from a population of explanted devices) may identify targets for immune-modulation that could increase the useful lifetime of individual implants.

1. Venail F, Sicard M, Piron JPet al. Reliability and complications of 500 consecutive cochlear implantations. *Archives of Otolaryngology - Head and Neck Surgery* 2008;134:1276-81.
2. Causon A, Verschuur C, Newman TA. Trends in cochlear implant complications: implications for improving long-term outcomes. *Otol Neurotol* 2013;34:259-65.
3. Bourdoncle M, Fargeot C, Poncet Cet al. Analysis and management of cochlear implant explantation in adults. *Eur Ann Otorhinolaryngol Head Neck Dis* 2020.
4. Nadol JB, Eddington DK, Burgess BJ. Foreign Body or Hypersensitivity Granuloma of the Inner Ear After Cochlear Implantation: One Possible Cause of a Soft Failure? *Otology and Neurotology* 2008;29:1076-84.
5. Seyyedi M, Nadol JB. Intracochlear Inflammatory Response to Cochlear Implant Electrodes in Humans. *Otology & Neurotology* 2014;35:1545-51.
6. Nadol JB, O'Malley JT, Burgess BJet al. Cellular immunologic responses to cochlear implantation in the human. *Hearing Research* 2014;318:11-7.
7. Ishai R, Herrmann BS, Nadol JBet al. The pattern and degree of capsular fibrous sheaths surrounding cochlear electrode arrays. *Hearing Research* 2017;348:44-53.
8. Bas E, Bohorquez J, Goncalves Set al. Electrode array-eluted dexamethasone protects against electrode insertion trauma induced hearing and hair cell losses, damage to neural elements, increases in impedance and fibrosis: A dose response study. *Hearing Research* 2016;337:12-24.
9. Needham K, Stathopoulos D, Newbold Cet al. Electrode impedance changes after implantation of a dexamethasone-eluting intracochlear array. *Cochlear Implants International* 2019;0:1-12.

10. Kamakura T, O'Malley JT, Nadol JB. Preservation of Cells of the Organ of Corti and Innervating Dendritic Processes Following Cochlear Implantation in the Human: An Immunohistochemical Study. *Otology and Neurotology* 2018;39:284-93.
11. Okayasu T, Quesnel AM, O'Malley JTet al. The Distribution and Prevalence of Macrophages in the Cochlea Following Cochlear Implantation in the Human: An Immunohistochemical Study Using Anti-Iba1 Antibody. *Otol Neurotol* 2020;41:e304-e16.
12. Bas E, Goncalves S, Adams Met al. Spiral ganglion cells and macrophages initiate neuro-inflammation and scarring following cochlear implantation. *Frontiers in Cellular Neuroscience* 2015;9.
13. Maddox PH, Jenkins D. 3-Aminopropyltriethoxysilane (APES): a new advance in section adhesion. *Journal of clinical pathology* 1987;40:1256-60.
14. Moreno B, Jukes JP, Vergara-Irigaray Net al. Systemic inflammation induces axon injury during brain inflammation. *Ann Neurol* 2011;70:932-42.
15. Christo SN, Diener KR, Bachhuka Aet al. Innate Immunity and Biomaterials at the Nexus: Friends or Foes. *BioMed Research International* 2015;2015.
16. Coelho NM, McCulloch CA. Contribution of collagen adhesion receptors to tissue fibrosis. *Cell Tissue Res* 2016;365:521-38.
17. Landgraeber S, Jäger M, Jacobs JJet al. The pathology of orthopedic implant failure is mediated by innate immune system cytokines. *Mediators Inflamm* 2014;2014:185150.
18. Galea I, Felton LM, Waters Set al. Immune-to-brain signalling: the role of cerebral CD163-positive macrophages. *Neurosci Lett* 2008;448:41-6.
19. Kzhyshkowska J, Gudima A, Riabov Vet al. Macrophage responses to implants: prospects for personalized medicine. *Journal of Leukocyte Biology* 2015;98:953-62.
20. Gurtner GC, Werner S, Barrandon Yet al. Wound repair and regeneration. *Nature* 2008;453:314-21.
21. Kendall RT, Feghali-Bostwick CA. Fibroblasts in fibrosis: Novel roles and mediators. *Frontiers in Pharmacology* 2014;5 MAY:1-13.
22. Sun X, Kaufman PD. Ki-67: more than a proliferation marker. *Chromosoma* 2018;127:175-86.
23. Anderson JM, Rodriguez A, Chang DT. Foreign body reaction to biomaterials. *Seminars in Immunology* 2008;20:86-100.
24. Mariani E, Lisignoli G, Borzì RMet al. Biomaterials: Foreign bodies or tuners for the immune response? *International Journal of Molecular Sciences* 2019;20.
25. Chung D, Kim AH, Parisier Set al. Revision cochlear implant surgery in patients with suspected soft failures. *Otology and Neurotology* 2010;31:1194-8.
26. Foggia MJ, Quevedo RV, Hansen MR. Intracochlear fibrosis and the foreign body response to cochlear implant biomaterials. *Laryngoscope Investig Otolaryngol* 2019;4:678-83.
27. Crowson MG, Semenov YR, Tucci DLet al. Quality of Life and Cost-Effectiveness of Cochlear Implants: A Narrative Review. *Audiol Neurootol* 2017;22:236-58.

Figure legends

Figure 1 *Clinical indicators of electrode migration concomitant with a deterioration in hearing.*

A. Electrode status and speech recognition scores over time. Scores for the BKB sentence test (in quiet) are shown for the cochlear implant alone (black line) and the hybrid (grey line) device [combined acoustic and electrical stimulation] post-implant. **B**. Impedance telemetry in common ground mode from activation until shortly prior to re-implantation. **C**. X-ray micrograph obtained 1-day post-implantation showing the intra-cochlear position of the electrode array. **D.** Electrode contact positions superimposed (black). **E**. Cochlear template adapted from Kawano et al 1996, defining the position of every quarter turn of the Organ of Corti, showing the points from the basal turn. The position of the electrode array post-implantation superimposed (black) based on the post-operative x-ray and the expected position of the migrated array before explantation superimposed (white) – showing four extra-cochlear electrodes.

Figure 2. *Explanted electrode with associated fibrotic tissue prior to tissue removal and after sectioning and histochemical staining to illustrate the variable cellular response and local organisation within the fibrotic tissue.*

Photographs of the full length of electrode array (**A**) showing fibrotic tissue enveloping the basal portion of the array. The insert in (A) identifies the four regions of tissue referred to in subsequent images and is shown at higher magnification in **B,** where the black arrows indicate tissue-covered electrode contacts and the numbers refer to the regions in C-F. **C-F** Low magnification (x4) images of sections representative of regions 1 to 4 respectively to illustrate the gross organisation of the tissue along its length. **G-N,** higher magnification (x40) images showing the variability in density of cells and volume of connective tissue across and within the regions. **G and H,** illustrate areas of loose connective tissue with sparsely distributed cells. **I** areas of dense, organised cells close to position of the electrode array. **J,** areas packed with cell nuclei and and dense connective tissue in **K** with aligned collagen fibres. **L-N,** inflammatory cells (arrows) including eosinophils (**L**), neutrophils (**M**), and foreign body giant cells (**N)**. Histochemical stains; haematoxylin and eosin, except G, K which are stained using MSB trichrome. Scale bar: C - F = 200 µm, G - N = 10 µm.

Figure 3. *Variable expression of cellular markers of macrophages and T cells within the explant tissue.*

Light microscopy images of tissue sections immunolabelled using **A**. anti-CD68, a marker of phagocytic macrophages. CD68-positive cells were observed at the edges of the tissue in close proximity to where the array was in all four regions. **B**. Anti-Interleukin 1β, a pro-inflammatory cytokine. **C**. Anti-CD163 a marker of anti-inflammatory macrophages. CD163-positive macrophages were observed in lower number (compared to CD68) and were mostly observed around the perimeter of the tissue. **D**. T-lymphocytes labelled with anti-CD3. Clusters of T cells were observed in region 4 in tissue furthest away from the array. Arrows highlight examples of positively labelled cells. Scale bar: 10 μm.

Figure 4. *Evidence of active tissue proliferation and angiogenesis.*

Light microscopy images of tissue sections immunolabelled using **A**. Anti-Ki-67 a marker of dividing i.e. proliferating cells. The majority of the Ki-67 positive cells were observed in regions of low cell density and high extracellular matrix. **B**. Vascular endothelial growth factor receptor-2 (VEGFR2) a marker of developing blood vessels i.e. angiogenesis. VEGFR2 expression was primarily observed in regions distal to the electrode array. **C**. Expression of alpha-smooth muscle actin (α-sma) clearly associated with blood vessel walls and **in D** α-sma positive cells indicating myofibroblasts that do not appear to be associated with vessels. Examples of positively labelled cells are indicated by arrows. Scale bar: 10 μm.

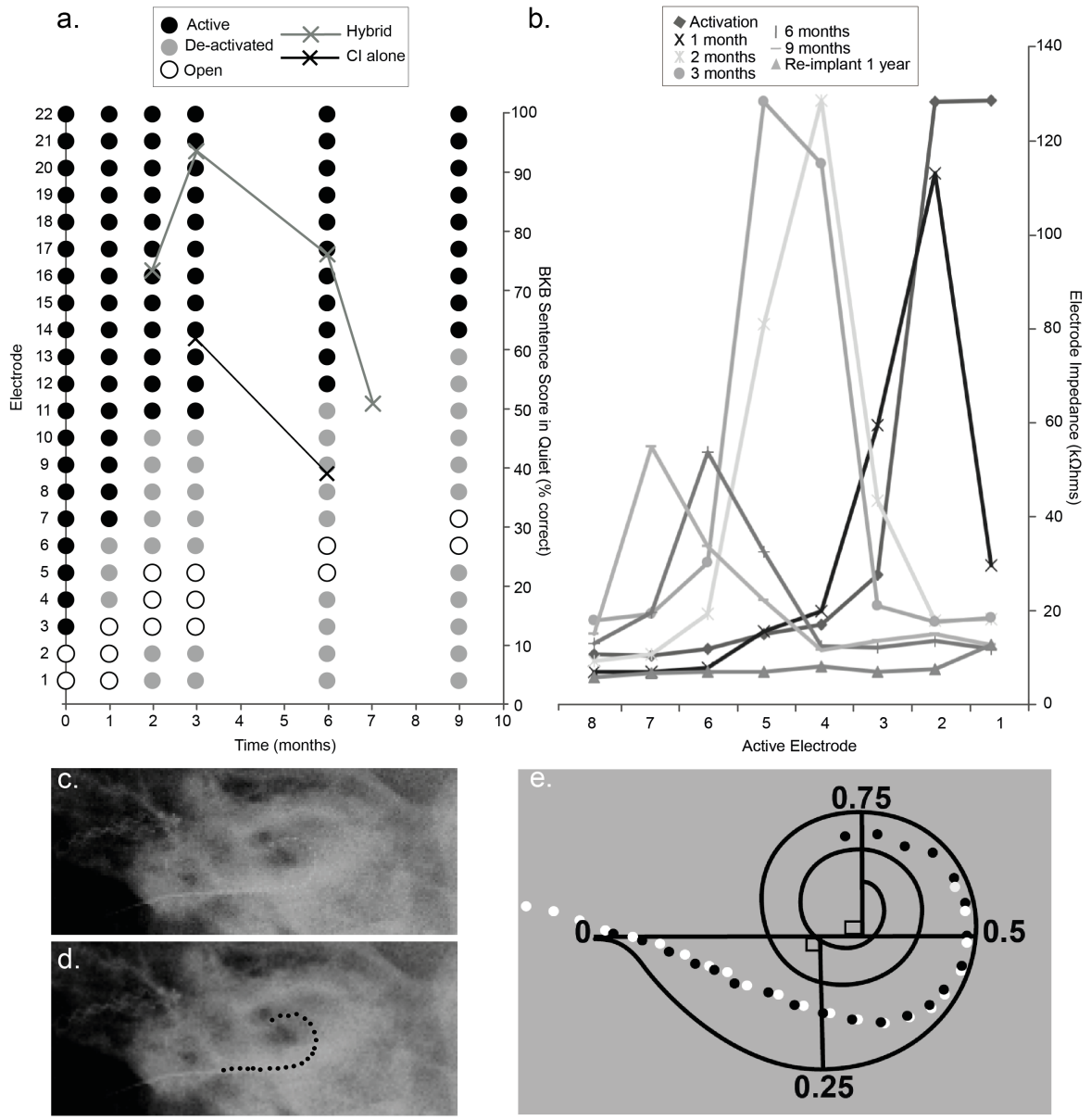
a.
Active
De-activated
Open
Hybrid
CI alone
Electrode
Time (months)
BKB Sentence Score in Quiet (% correct)
b.
Activation
1 month
2 months
3 months
6 months
9 months
Re-implant 1 year
Active Electrode
Electrode Impedance (kΩhms)
c.
d.
e.
0.75
0
0.5
0.25

Figure 1

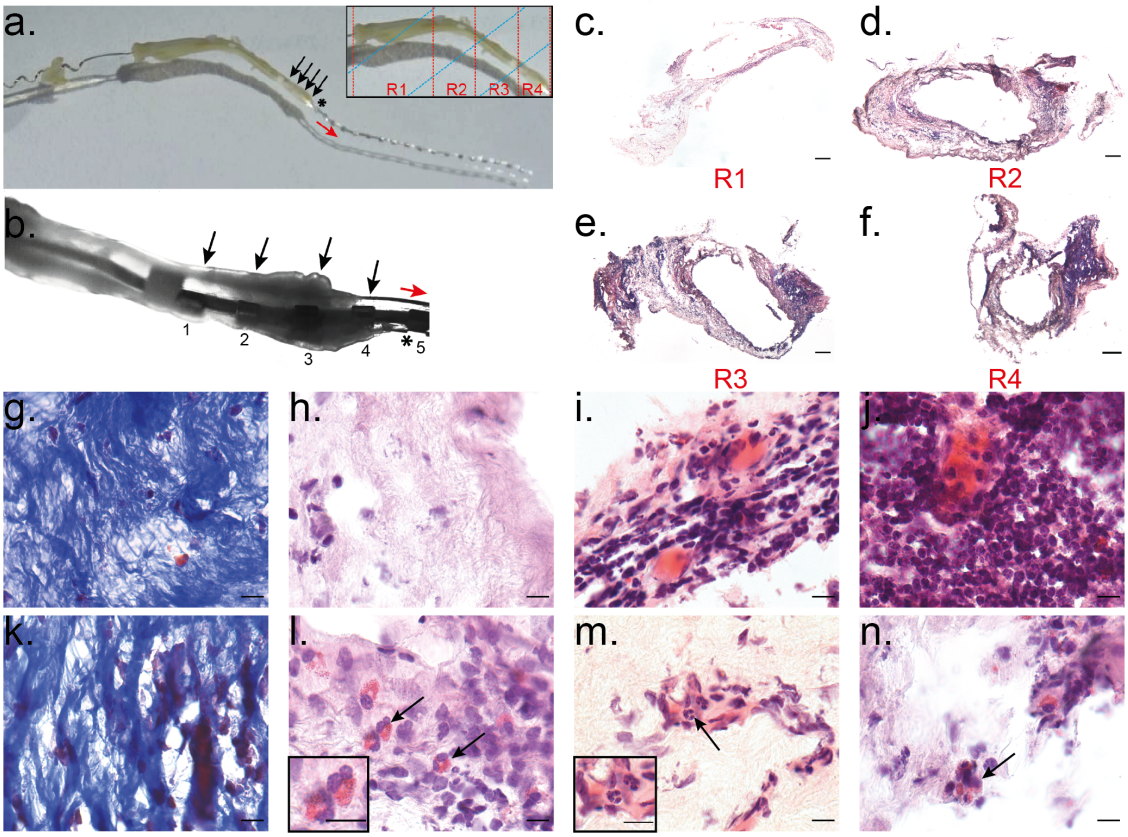

Figure 2

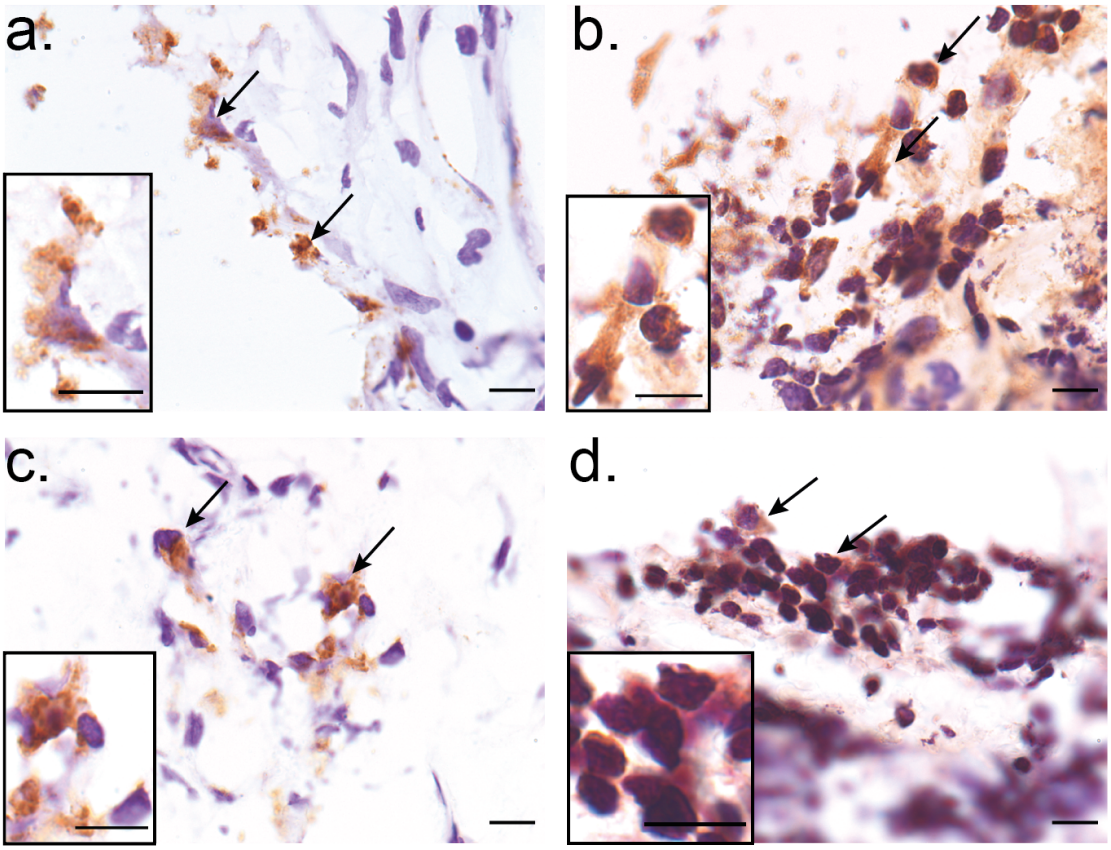

Figure 3

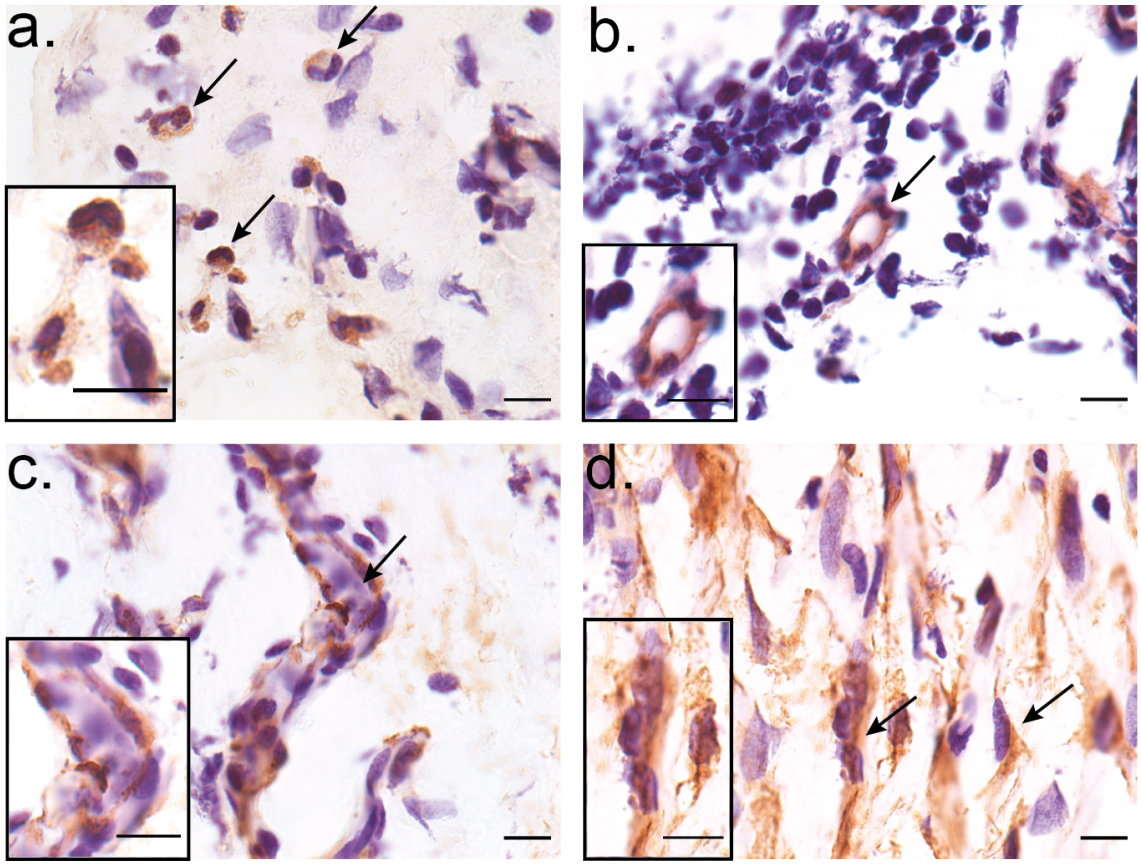

Figure 4

Table (supplementary)

Target cell/tissue	Antibody	Manufacturer	Host species	Dilution	Antigen Retrieval	Blocking agent	Secondary antibody
Macrophage	CD68	Abcam (ab783)	Mouse	1:100	citrate buffer	Normal goat serum 1.5% in PBS	Goat anti-mouse 1:1000 (BA-9200)
Macrophage	CD163	Abcam (ab182422)	Rabbit	1:250	citrate	Normal goat serum 1.5% in PBS	Goat anti-rabbit 1:200
Dividing cells (proliferation)	Ki-67	Abcam (ab15580)	Rabbit	1:600	citrate buffer	Normal goat serum in 0.01% TX100 0.25% BSA	Goat -anti Rabbit 1:200 in 0.01% TX100 0.25% BSA
Blood vessels, myofibroblasts	α-SMA (anti-actin alpha smooth muscle clone 1A4)	Sigma	Mouse	1:50,000	citrate buffer	Normal goat serum 1.5%	Goat -anti mouse 1:200 in 0.01% TX100 0.25% BSA
T-Lymphocytes	CD3	Dako	Rabbit	1:200	citrate buffer	Normal goat serum 1.5%	Goat anti-rabbit 1:200
IL-1β (Pro-inflammatory cytokine)	IL-1β	Peprotech	Rabbit	1:50	citrate buffer	Normal goat serum 20%	Goat anti-rabbit 1:200
Vasculogenesis	VEGF-R2	Cell signalling Technology (55B11)	Rabbit	1:600	EDTA with tween	Normal goat serum 5%	Goat anti-rabbit 1:200 in TBS Tween

Supplementary Table 1. Details of the antibodies and methods used for the immunohistochemical labelling of the tissue